

Effect of temperature on MRPC with pad read-outs^{*}

DING Wei-Cheng(丁卫撑)^{1,2;1)} WANG Yi(王义)^{2;2)} TUO Xian-Guo(庹先国)^{1;3)}
 CHENG Huang-Shan(陈黄山)² WANG Jing-Bo(王景波)² WANG Min(王敏)¹

¹ Chengdu University of Technology, Key Laboratory of Applied Nuclear Technology in Geosciences, Chengdu 610069, China

² Department of Engineering Physics, Tsinghua University, Key Laboratory of Particle & Radiation Imaging,
 Ministry of Education (Tsinghua University), Beijing 100084, China

Abstract: To obtain a quantitative understanding of the influence of temperature on the performance of multi-gap resistive plate chambers (MRPCs), we have tested the performance of a 10-gap, 12-pad, $2 \times 2 \times 12 \text{ cm}^2$ active area MRPC at different temperatures with cosmic rays. Presented are results from measurements of high-voltage scans, noise rate, dark current, streamer, time resolution, count rate, charge spectrum, and detection efficiency. The test results show that the MRPC performance is significantly affected by temperature arising from the temperature-dependence of the glass resistivity.

Key words: MRPC, rate capability, time resolution, efficiency, temperature testing

PACS: 12.38.Qk, 29.40.Cs **DOI:** 10.1088/1674-1137/37/9/096001

1 Introduction

Good timing characteristics and high detection efficiency [1] of the multi-gap resistive plate chamber (MRPC) make it a favorable candidate as a time-of-flight (TOF) detector in heavy-ion collision experiments, such as ALICE, FOPI, HADES, HARP and STAR [2–6]. The Compressed Baryonic Matter (CBM) experiment, proposed at the future FAIR accelerator facility (GSI, Germany), is to investigate strongly interacting matter under extremely high net baryon densities and moderate temperatures [7]. In the current design for the hadron identification, consideration has turned to using a TOF system based on MRPCs. However, concerning the outer part of the TOF wall (rate region 4), a high rate capability up to $0.5\text{--}1.5 \text{ kHz/cm}^2$ is required for the MRPCs. To achieve this goal, the CBM group has discussed that it is ready to work on increasing the temperature of the MRPCs as a means to increase the count rate [7–9]. There have been a number of studies on MRPCs indicating that performance is significantly affected by temperature [9, 10]. To understand quantitatively that dependence, we tested a 10-gap, 12-pad MRPC at different environmental temperatures with cosmic rays and X-ray.

2 Cosmic ray test system setup

The tests were performed on a 12-pad timing MRPC whose cross-section is illustrated in Fig. 1. The detector is an MRPC with 10 gaps consisting of a stack of resistive (glass, bulk resistivity $5 \times 10^{12} \Omega/\text{cm}^2$) plates with nylon fishing line (0.25 mm diameter) used as spacer between the glass plates to maintain gap size. The high voltage (HV) is applied to the graphite HV electrode (surface resistivity $5 \text{ M}\Omega/\text{cm}^2$) on the external surfaces of the outer glass plates. The thickness of the inner glass plate is 0.7 mm and the outer glass plate is 1.1 mm. The sensitive area of the MRPC is $12 \text{ cm} \times 4 \text{ cm}$. There are twelve $2 \text{ cm} \times 2 \text{ cm}$ copper readout pads with intervals of 2 mm. Each pad is connected with a low-noise fast amplifier. A layer of Mylar (0.18 mm thick) is used to insulate the HV electrodes from the copper readout pads. The thickness of the outboard read-out printed circuit board (PCB) is 0.8 mm. The middle readout PCB is composed of three layers with a read-out pad in the middle; its thickness is 1.6 mm. A gas mixture of freon/iso-butane/SF₆ (96%/1%/3%) at normal pressure flows through the chamber, which is located in a gas sealed aluminum box.

Received 26 November 2012, Revised 20 December 2012

* Supported by National Natural Science Foundation of China (41204133), Young Backbone of Scientific Research Plan of CDUT and Projects of International Cooperation and Exchanges NSFC (11020101059)

1) E-mail: dingweicheng@cdut.cn

2) E-mail: yiwang@tsinghua.edu.cn

3) E-mail: txg@cdut.edu.cn

©2013 Chinese Physical Society and the Institute of High Energy Physics of the Chinese Academy of Sciences and the Institute of Modern Physics of the Chinese Academy of Sciences and IOP Publishing Ltd

To effect changes in the temperature of the MRPC, an electric heating belt is wrapped around the gas box. The set-up is depicted in Fig. 2. Heating of the belt is controlled by a temperature stabilization system. Several temperature sensors placed in the box monitor temperature; an average of the readings is used to estimate the MRPC temperature. With accuracy generally within $\pm 1^\circ\text{C}$, the encased MRPC can be maintained at a steady temperature to within these limits. We also put two temperature sensors in the front-end electronics (FEE) box to measure the temperature of the FEE work environment. We heated the upper and lower surface of the test box with the same electric heating belt. Thus, the surface temperature for the MRPC is the same, putting the temperature sensors only on the upper surface and both sides of the MRPC.

A Max3760ESA is used as an FEE Pre-amplifier. Both time (measured by a CERN Mod.V775AC) and charge data (measured by a CERN Mod.V792AC) were taken from each of the MRPC extremities using a cos-

mic ray test system. The trigger system, a schematic of which is given in Fig. 3, consists of five scintillation counters. The coincident outputs of photon multipliers tubes (PMTs), PMT1 and PMT5, are used as the common stop signal of the TDC and the gate signal of the QDC. The area of scintillator 4 and scintillator 5 is $3.5\text{ cm} \times 2\text{ cm}$ which is smaller than the area of two pads. Thus, when cosmic rays pass through scintillator 4 (PMT6) and scintillator 5 (PMT7), these will also pass through the two MRPC pads. The ratio of the coincident counts of MRPC over PMT1–PMT7 constitutes the efficiency of MRPC.

The dark current of the MRPC after applying HV is read out directly from a CAEN N471A (sensitivity of 1nA) that supplies the HV. The output signals from the MRPC readout pads go through the FEE box: amplifier, discriminator (the threshold corresponds to 50 mV), shaper, and then the scaler (CERN Mod.N145) to measure the noise rate.

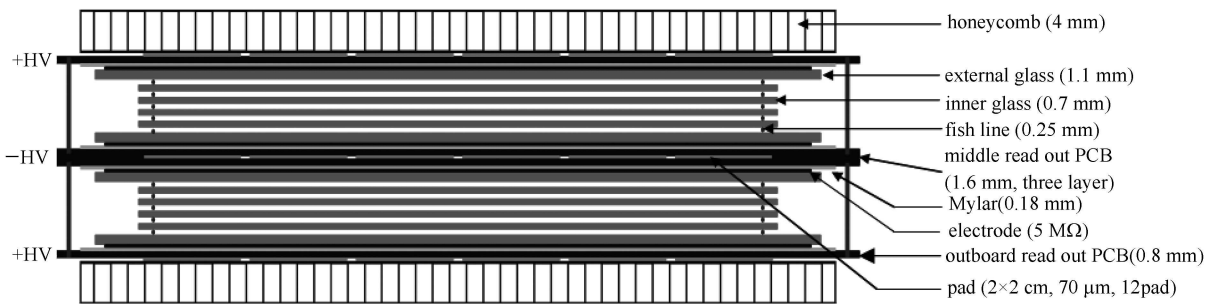


Fig. 1. The structure of the 10-gap, 12-pad MRPC.

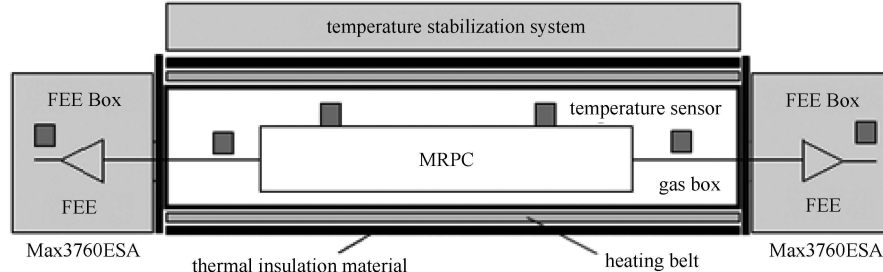


Fig. 2. Schematic of the constant temperature testing box.

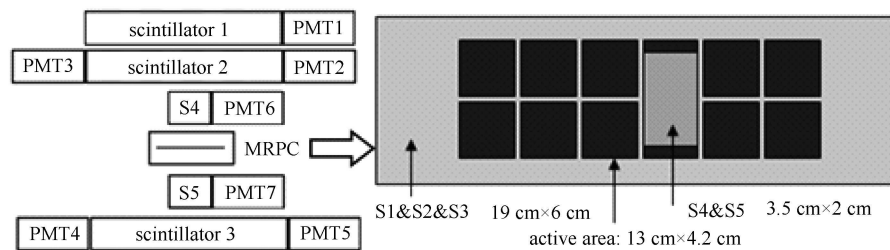


Fig. 3. The trigger of cosmic ray test system.

3 Test result

Before starting the test, the MRPCs were conditioned under HV for a few hours to reach a stable, low dark-rate working status. At an HV of ± 69 kV and 50 mV threshold, we used a gas mixture of freon/isobutane/SF₆ (96%/3%/1%). When we performed the temperature test, we kept the temperature stable for every test point for at least 12 h. The temperature was increased from 25 °C to 60 °C at 5 °C degree intervals. The temperature in the FEE box changed as the temperature in the MRPC test box changed. Fig. 4 shows the result of the temperature changes in the FEE box vs. the temperature changes in the MRPC test box. From Fig. 4 we can see that over the range 35–60 °C, the temperature in the FEE box changes slowly as the temperature in the MRPC test box changes. Thus, we infer that temperatures in the test box weakly influence temperatures in the FEE box.

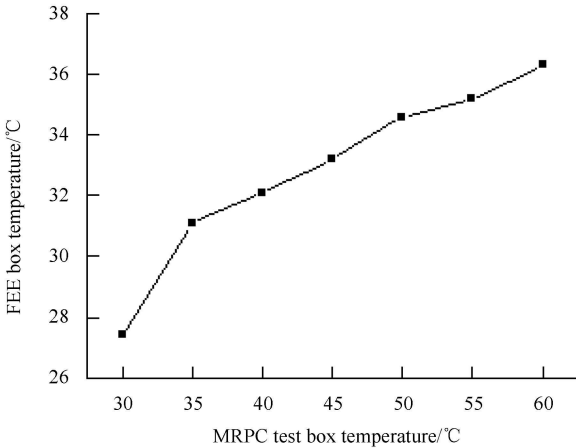


Fig. 4. MRPC test box temperature vs. FEE box temperature.

3.1 Slewing correction and HV scan

To find the optimum operating voltage of the counters, the efficiency and time resolution were scanned as a function of HV under cosmic ray testing. The efficiencies are always determined by the valid rates recorded

by the scintillators as well as the MRPCs. These results are summarized after Gaussian fitting in Fig. 5(a)–(c). Fig. 5(a) shows the PMT reference time resolution, which is used to extract the pure-start resolution, and Fig. 5(b) shows the MPRC total time resolution, from which the pure-stop resolution is obtained by subtracting the start resolution. The time resolution is calculated by characterizing the distribution of the time difference between the MRPCs and PMT:

$$\sigma_{\text{TOF}} = \sqrt{\sigma_{\text{MRPC}}^2 - \sigma_{\text{PMT}}^2} \times 35 \text{ ps.} \quad (1)$$

Figure 5(c) shows the MRPC efficiency and time resolution under different HVs at room temperature (25 °C). It can be seen that time resolutions of 81 ps can be obtained with efficiencies larger than 94% at a working voltage of ± 6.9 kV. Thus, we take ± 69 kV as the HV work point at different temperatures.

3.2 Noise and dark current

The noise rate of the MRPC at different environment temperatures is measured, and the data is shown in Fig. 6. There, we can see that noise is stable when temperatures are below 40 °C but quickly increases above 40 °C. This plot indicates that the noise increases exponentially with the temperature. Thus, we conclude that the best operating environment for the MRPC should be below 40 °C with low noise.

The results of the MRPC dark current vs. temperature in the cosmic ray testing before high-rate X-ray irradiation (Fig. 7) show that the dark current is flat versus the temperature over 25–50 °C. In contrast, Fig. 6 shows a strong dependence of the noise rate on the temperature. Why are the noise rates? and dark currents? changes not in parallel? Because SF₆ can effectively inhibit avalanche generation, so that the MRPC output noise signal is small, just over threshold. The effect of noise on dark current is weak.

Temperature not only affects MRPC gas but also affects the electrode glass and the insulating properties of the insulating material. From the dark current test result

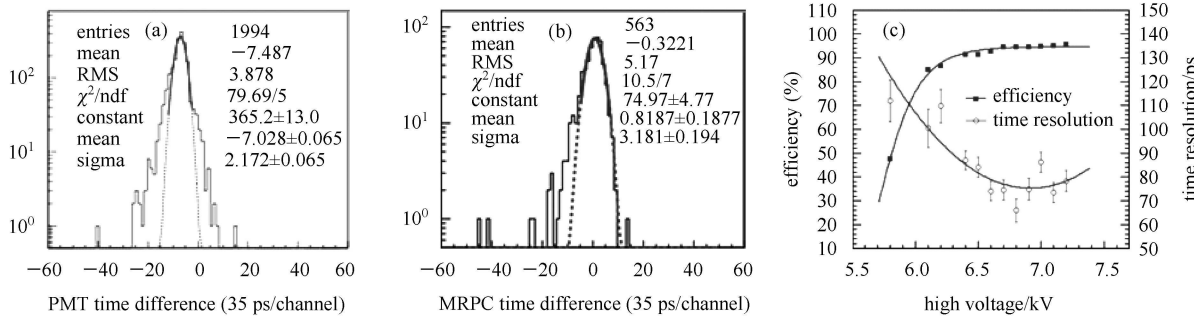


Fig. 5. (a) PMT time resolution; (b) MRPC time resolution (HV=±6.9 kV); (c) Efficiency and time resolution as a function of high voltage.

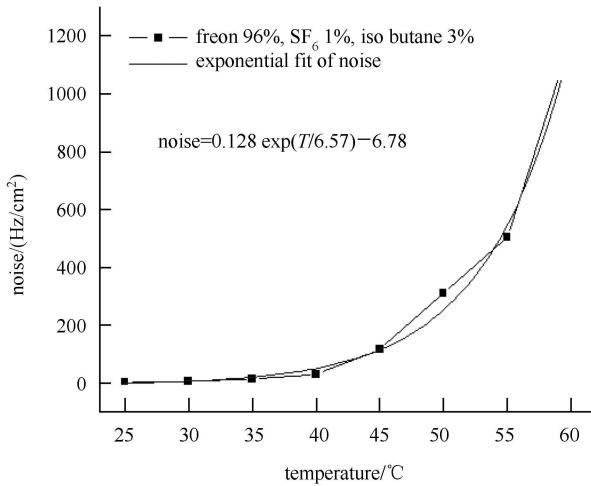


Fig. 6. Noise vs. temperature ($HV=\pm 6.9 \text{ kV}$).

which is shown on Fig. 7 we can conclude that the temperature effect on the insulating material such as nylon fish line, Mylar insulation, is weak.

Since the electrode glass has inherent thermal noise, the thermal noise voltage of the mean square value (Vn^2) satisfies the following equation:

$$Vn^2 = 4k \cdot B \cdot T \cdot R, \quad (2)$$

where k is Boltzmann constant ($1.37 \times 10^{-23} \text{ J/K}$), T is absolute temperature (K), R is glass internal resistance (Ω), B is band width (Hz).

R satisfies the following equation:

$$R = \rho^0 \cdot e^{bt} \cdot d / A, \quad (3)$$

where ρ^0 is resistivity, b is fitting parameter and it is a negative number, t is temperature ($^{\circ}\text{C}$), d is glass thickness, A is glass area. So we can get the following equation:

$$Vn^2 = 4kB(273.15+t)\rho^0 \cdot e^{bt} \cdot d / A. \quad (4)$$

Therefore, the temperature increase will increase the output of the thermal noise of the electrode glass, and then affect MRPC noise count rate. This is also one of the reasons why the noise rates? and dark currents? change are not in parallel.

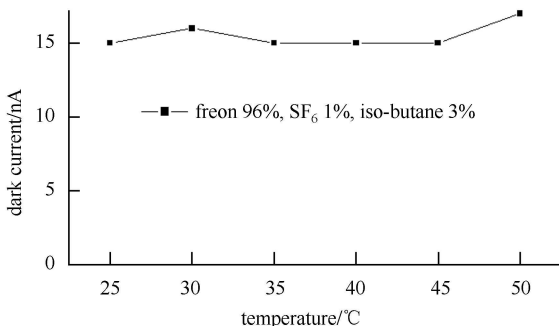


Fig. 7. Dark current vs. temperature ($HV=\pm 6.9 \text{ kV}$).

3.3 Charge distribution and time resolution

We also made a thorough experimental study of the effect of temperature on signal amplitude. We performed the test twice and present just the average of the test results. Fig. 8 shows the relationship between temperature and the mean charge which cut streamer signals; Fig. 9 shows the relationship between the streamer and temperature under the same test conditions. From these results we can see that the signal amplitude increases as temperature increases. The error bars are the systematic uncertainties obtained from multiple independent measurements of these quantities. Also, both Figs. 8 and 9 exhibit a point-to-point staggering which may indicate some systematic uncertainties in the data caused by the experimental setup or data collection.

The pressure of the gas mixture remains the same when the temperature shifts because the working gas is of flow gas type. Thus, gas temperature increases will lead to a decrease in the gas density inside the box, lengthening the electron mean free path; e-collisions with gas molecules will increase access to energy, which increases the ionization cross section, that is, the effective Townsend ionization coefficient increases. In consequence, the number of ions increases allowing then for an increase in gas amplification. This sequence offers a physical explanation for the increased MRPC efficiency with increasing temperature. In a given temperature range, the gas avalanche amplification factor depends on E/ρ . The gas density decreases with temperature rises. To ensure constant gain, the electric field should be reduced, that is, the applied HV should be decreased.

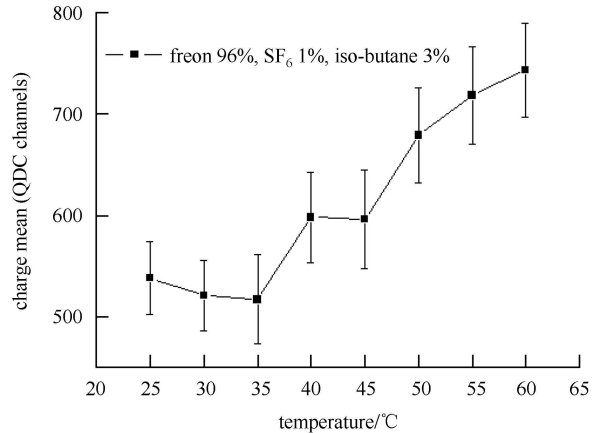


Fig. 8. Charge mean vs. Temperature ($HV=\pm 6.9 \text{ kV}$).

Timing measurements were performed by the method described in Section 3 under the effective applied voltage and working temperature. At each temperature test point, we performed cosmic ray tests for two days to ensure we can record more than 1000 events. We conducted the test twice for each temperature.

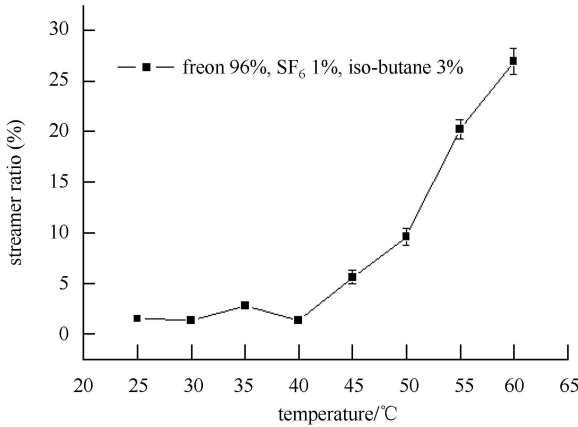


Fig. 9. Streamer ratio vs. temperature ($HV = \pm 6.9$ kV, mean of all pads).

The time resolution results with slewing corrections are presented in Fig. 10. Remarkably, temperature exerts discernible effects on time resolution. The results shown in Fig. 10 indicate that the time resolution improves as temperature rises, which seems rather strange. With an increase in temperature, the electron mean free path becomes large which does not favor any time resolution improvement. Also, the detector gain will increase with increasing temperature at the same HV and thus decrease the time resolution. Fig. 8 shows that the signals are getting larger with temperature increasing. Larger signals always lead to better timing with leading edge discrimination. However, increasing temperature increases the electron speed, which helps to reduce the shaping time of the forefront of the time signal, thus improving the time resolution. Uncertainties of the system will also affect the time resolution results. Because too few events were measured, statistical fluctuation errors can have a greater impact on results. A beam test should be planned in a further study to obtain more accurate results.

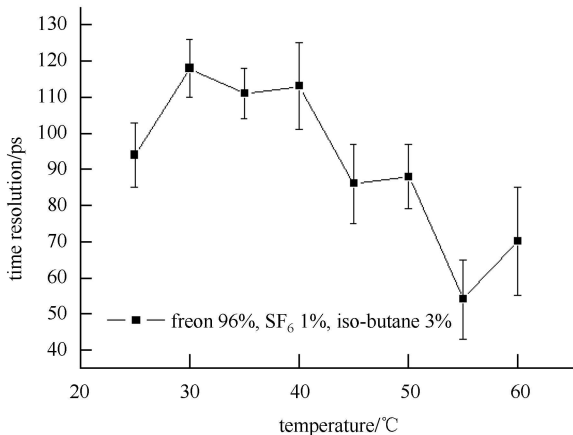


Fig. 10. Time resolution vs. temperature ($HV = \pm 6.9$ kV).

3.4 The rate tests undertaken with an X-ray source

An illustration of the test facility setup for this test is given in Fig. 11. The threshold is 50 mV with mixture of freon/iso-butane/SF₆ (96%/1%/3%) as working gas being used. We use X-ray for this test. Lead (Pb) of thickness 10 mm with a 2 mm×2 mm hole in the center is used as a collimator, which just covers one pad of the MRPC. During the test, we changed the X-ray intensity and read the rate from the pad and the current of the MRPC.

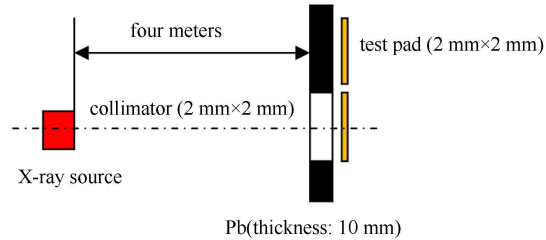


Fig. 11. Rate test structure.

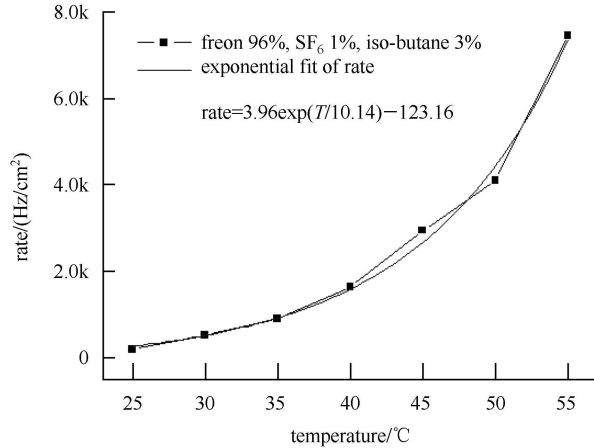


Fig. 12. Rate capability vs. temperature ($HV = \pm 6.9$ kV).

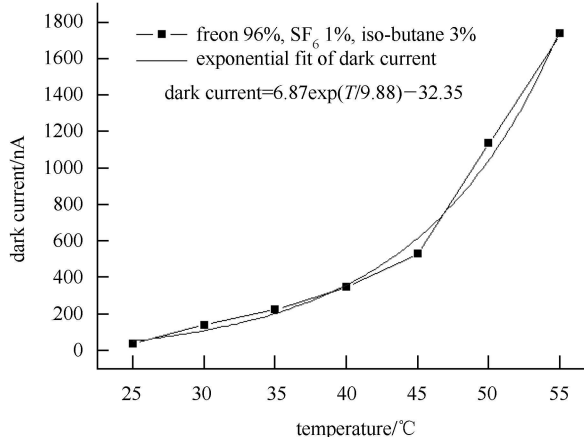


Fig. 13. Dark current vs. temperature in the conditions of MRPC count rate saturated under high-rate X-ray irradiation ($HV = \pm 6.9$ kV).

The X-ray source rate was increased until the MRPC count rate saturated. Additional increases of the source rate did not result in additional increases in the MRPC count rate. These saturation values of the MRPC count rates are plotted versus the temperature in Fig. 12. This plot indicates that the maximum possible MRPC count rate increases exponentially with the temperature.

Figure 13 shows the results of MRPCs dark current vs. temperature in the conditions of MRPC count rate saturated under high-rate X-ray irradiation. Also the results indicate an increased current with increasing temperature.

4 Conclusion

Under cosmic-ray tests of an MRPC with pad readouts, noise rate rises approximately exponentially, the

dark current changes little and time resolution is improved as temperature increases. However, the dark current rises approximately exponentially in high-rate X-ray tests. It was demonstrated in timing the MRPC that a 25 °C temperature increase improves the count rate capability by one order of magnitude, extending the applicability of timing RPCs made with industrial flat common glass to much larger counting rates merely by a moderate warming of the detector. In consequence, a study of the practical use of warming an MRPC would be interesting as it provides an easy means to extend the counting rate capability while retaining the practical advantages of using industrial flat glass in construction. Naturally, further research is required on issues like temperature control of large RPC systems, detector aging and materials? compatibility in higher temperature conditions.

References

- 1 Zeballos E C, Crotty I, Williams M et al. Nucl. Instrum. Methods A, 1996, **374**: 132
- 2 Akindinov A, Alici A, Antonioli P et al. Nucl. Instrum. Methods A, 2009, **602**: 709
- 3 Schüttauf A. Nucl. Instrum. Methods A, 2004, **533**: 65
- 4 Alvarez-Pol H, Alves R, Blanco A et al. Nucl. Instrum. Methods A, 2004, **535**: 277
- 5 Blanco A, Cabanelas P, Belver D et al. Nucl. Instrum. Methods A, 2009, **602**: 691
- 6 WANG Yi, LI Yuan-Jing, CHENG Jian-Ping et al. Nucl. Instrum. Methods A, 2005, **538**: 425
- 7 Letter of Intent for the CBM Experiment, Darmstadt, Germany, 2004
- 8 CBM collaboration. CBM progress report 2009, March 2010, 37
- 9 Gonza'lez-Díaz D, Belver D, Blanco A et al. Nucl. Instrum. Methods A, 2005, **555**: 72
- 10 ZHAO Y E, WANG X L, LIU H D et al. Nucl. Instrum. Methods A, 2005, **547**: 334